CSI Feedback for Distributed MIMO

Gilwon Lee, Md Saifur Rahman, and Eko Onggosanusi
Standards and Mobility Innovation Lab, Samsung Research America, Plano, TX 75023, USA
E-mail: {gilwon.lee, md.rahman, eko.o}@samsung.com

2022 IEEE Wireless Communications and Networking Conference (WCNC) | 978-1-6654-4266-4/22/$31.00 ©2022 IEEE | DOI: 10.1109/WCNC51071.2022.9771853

***Abstract*—In this paper, we consider a distributed multi-input-multi-output (D-MIMO) system wherein multiple radio remote heads (RRHs) distributed in a cell are connected with a single baseband unit. To enable coherent joint transmission from multiple RRHs in the D-MIMO system, we propose several channel state information (CSI) codebooks as candidates for enhancements in the context of 3rd Generation Partnership Project (3GPP) 5G New Radio (NR) standardization. The proposed codebooks are developed based on the 5G Release-16 Type-II CSI codebook framework. In addition, we propose dynamic RRH selection (DRS) methods that are able to obtain performance gain and reduce the amount of feedback by sending the CSI only for the selected RRHs having dominant channel qualities. System-level simulation (SLS) results under realistic scenarios are provided to validate the potential of the proposed CSI codebooks and DRS methods.**

I. Introduction

The channel state information (CSI) acquisition at the base station (BS) is one of the critical components to support MIMO communication efficiently. For CSI acquisition, the 3rd Generation Partnership Project (3GPP) has standardized the CSI feedback schemes as MIMO technologies have evolved from 4G full dimension MIMO to 5G new radio (NR) MIMO. In 5G NR MIMO, there are two types of CSI feedback mechanisms, supported based on low low-resolution (Type-I) and high-resolution (Type-II) codebooks, respectively, and for two-dimensional (2D) active antenna (AA) arrays at the BS capable to support 3D beamforming in vertical and horizontal domains. Different types of CSI feedback schemes are designed to offer various use cases and considering different levels of user equipment (UE) capabilities [1].

In 5G NR Type-I CSI, up to four neighboring Discrete Fourier Transform (DFT) vectors can be chosen from a predefined set of DFT vectors, where this selection is performed in a wideband (WB) manner, i.e., the chosen DFT vectors are for the entire frequency band comprising multiple subbands (SBs). The dominant channel direction is expressed via single DFT vector selection per subband (SB), where this per SB selection is from the up to four neighboring DFT beams. Thus, the Type-I CSI incurs low feedback overhead, but it works reasonably well for single user MIMO (SU-MIMO) since capturing a dominant direction of the channel for a given UE is usually sufficient and the system performance is less sensitive to precise precoder selection at the base station (BS). For multiuser- (MU-)MIMO transmission, however, high-resolution CSI capturing multiple dominant directions of the channel is essential to suppress inter-user interference by precisely selecting precoder at the BS for spatial multiplexing

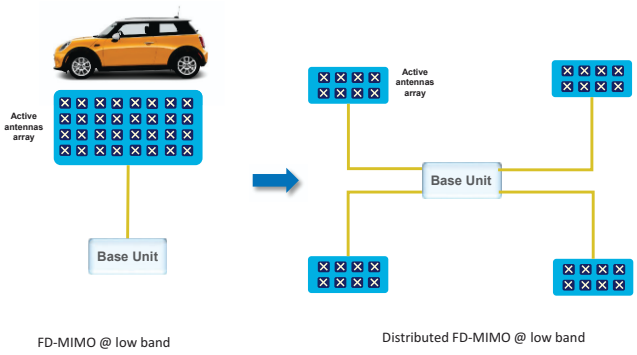

Figure 1. A necessity of distributed MIMO at low band scenarios.

amongst different UEs, which is why Type-II CSI has been developed.

The 5G NR Type-II CSI has been designed based on the concept to represent an eigenvector of the channel via linear combination (LC) of chosen basis vectors and their corresponding coefficients. For channels having a high rank, multiple dominant eigenvectors of the channel are reported, each of which is quantized via the LC codebook independently but based on a common set of basis vectors. In Release 15 (Rel-15) Type-II CSI feedback, spatial domain (SD) basis vectors are reported in a WB manner, i.e., one common basis set is reported for all SBs and the coefficients corresponding to the common basis vectors are quantized for each SB and reported to the BS [2]. In addition to a SD basis, frequency domain (FD) basis vectors are additionally introduced in the Rel-16 Type-II CSI to further reduce the CSI feedback overhead by compressing channel coefficients in both spatial and frequency domains [3], exploiting the channel correlation across SBs.

Recently, low frequency bands (sub-1GHz) previously allocated for 4G deployments and those used for digital TVs are being re-farmed for 5G NR to use another carrier frequency in addition to mid and high frequency bands [4]. The low frequency bands have several beneficial properties such as wide coverage thanks to the low path loss and good quality of channels having smaller Doppler effect, and thus it is expected to be useful to serve as an anchor carrier to support or assist multiple small cells that are served using mid or high frequency bands. However, the small bandwidth of low frequency bands limits the capacity in frequency resource domain. Therefore, another resource domain such as multiple antennas (spatial) becomes crucial to enhance communications in low frequency bands. In order to deploy the conventional

full dimension MIMO or massive MIMO using low frequency bands, however, an extremely large physical antenna space is needed, as shown in Fig. 1, due to the large wavelength at the low frequency bands, which is infeasible in real deployments. This motivates a necessity of distributing antennas at multiple remote radio heads (RRHs), leading to distributed MIMO (D-MIMO) systems.

D-MIMO has been studied widely in academia since mid of 2000s [5], and it is also linked to the notion of cell-free network where multiple distributed antenna access points form a single massive MIMO system [6]. In the prior work on the cell-free massive MIMO, however, time-division duplex (TDD) has been the main consideration, and thus the channel reciprocity can be exploited for CSI acquisition at the BS through estimating uplink reference signals (UL RS) [7], [8]. For frequency-division duplex (FDD) bands that are mainly available at low frequency bands (e.g. below 1 GHz), however, the CSI feedback for the traditional centralized MIMO architecture needs to be enhanced to that for the D-MIMO architecture. One may consider the Rel-15 Type-I multi-panel (MP) codebook for D-MIMO systems [9], but it is not applicable to a general D-MIMO system since the supported antenna array structures are restricted to either 2 or 4 of identical and collocated antenna panels, allowing only a common beam selection across panels and inter-panel co-phase coefficient feedback. In this paper, we consider the CSI feedback in the context of 3GPP standardization, including CSI codebooks and dynamic RRH selection methods, in order to support CSI acquisition in a general D-MIMO FDD system.

II. NR Release-16 Type-II CSI Codebook

Let $\tilde{\mathbf{H}}[k]$ be an $N \times N_{\mathrm{RX}}$ DL channel between BS and UE at SB $k = 1, \cdots, K$, where N_{RX} is the number of receive antenna ports at the UE. The UE estimates the DL channel $\tilde{\mathbf{H}}[k]$ for each SB $k = 1, \cdots, K$, and find its V dominant channel directions, where $V \leq \min(N, N_{\mathrm{RX}})$. With singular value decomposition for $\tilde{\mathbf{H}}[k]$, the left singular vectors of $\tilde{\mathbf{H}}[k]$ corresponding to the dominant singular values can be derived to find the V dominant channel directions. For a given $\nu = 1, \cdots, V$, we can form the $N \times K$ dominant channel matrix $\mathbf{H}^{(\nu)}$ composed of the ν-th dominant left singular vector of $\tilde{\mathbf{H}}[k]$ for each SB $k = 1, \cdots, K$. That is, the k-th column of $\mathbf{H}^{(\nu)}$ corresponds to the ν-th dominant channel direction of $\tilde{\mathbf{H}}[k]$ for SB k. Then, the UE generates CSI for the dominant channel matrix $\mathbf{H}^{(\nu)}$ using the Rel. 16 Type-II CSI codebook, which is given by: $\mathbf{H}^{(\nu)} \simeq \mathbf{W}^{(\nu)} = \mathbf{W}_1 \mathbf{W}_2 \mathbf{W}_f^H$, where $\mathbf{W}_1$ and $\mathbf{W}_f$ are $N \times 2L$ and $K \times M$ basis matrices composed of SD and FD basis vectors, respectively, and $\mathbf{W}_2$ is an $2L \times M$ coefficient matrix corresponding to SD and FD vector pairs. Here, $N, K, 2L$, and M are the numbers of antenna ports (or CSI-RS ports) at the BS, SBs, SD basis vectors comprising columns of $\mathbf{W}_1$, and FD basis vectors comprising columns of $\mathbf{W}_f$, respectively [10].

The SD basis vectors are selected from a pre-defined set of 2D DFT basis vectors according to the configured 2D BS antenna layout comprising of $N_1 \times N_2$ dual-polarized antenna ports (i.e., $N = 2N_1N_2$). Specifically, a 2D orthogonal DFT basis is a set of N_1N_2 DFT beams $\{\mathbf{v}_{k_1+O_1l_1,k_2+O_2l_2} : l_1 \in \{0, 1, \cdots, (N_1-1)\}$ and $l_2 \in \{0, 1, \cdots, N_2-1\}\}$ for a given pair of (k_1, k_2), where $k_1 \in \{0, 1, \cdots, O_1 - 1\}$ and $k_2 \in \{0, 1, \cdots, O_2-1\}$. The oversampled DFT codebook comprises DFT beams: $\mathbf{v}_{l_1,l_2} = [\mathbf{u}_{l_2} \; e^{j\frac{2\pi l_1}{O_1N_1}}\mathbf{u}_{l_2} \; \cdots \; e^{j\frac{2\pi l_1(N_1-1)}{O_1N_1}}\mathbf{u}_{l_2}]^T$, where $\mathbf{u}_{l_2} = [1 \; e^{j\frac{2\pi l_2}{O_2N_2}} \; \cdots \; e^{j\frac{2\pi l_2(N_2-1)}{O_2N_2}}]$, $0 \leq l_1 \leq O_1N_1-1$, and $0 \leq l_2 \leq O_2N_2-1$, and O_1 and O_2 are the oversampling factors in the first and second dimensions, respectively. Thus, the pre-defined 2D DFT basis set has $O = O_1O_2$ orthogonal bases for the whole N_1N_2-dimensional space and one orthogonal basis is selected among them. Once an orthogonal basis is selected, L out of the N_1N_2 orthogonal vectors are commonly selected for both antenna polarizations and layers to construct $\mathbf{W}_1 = \begin{bmatrix} \mathbf{B} & \mathbf{0} \\ \mathbf{0} & \mathbf{B} \end{bmatrix}$ where $\mathbf{B} = [\mathbf{b}_0 \; \mathbf{b}_1 \; \cdots \; \mathbf{b}_{L-1}]$ is the basis matrix composed of the selected L SD basis vectors.

Similar to the SD, the FD basis vectors are selected from a pre-defined set of 1D DFT vectors according to the configured number of SBs. Specifically, an 1D orthogonal DFT basis is a set of K DFT beams $\{\mathbf{w}_{m+O_3l} : l \in \{0, 1, \cdots, (K-1)\}\}$ for given m, where $m \in \{0, 1, \cdots, O_3 - 1\}$. The oversampled DFT codebook comprises DFT vectors $\mathbf{w}_k = [1 \; e^{j\frac{2\pi k}{O_3K}} \; \cdots \; e^{j\frac{2\pi k(K-1)}{O_3K}}]$, where $0 \leq k \leq O_3K - 1$ and O_3 is the oversampling factor for FD DFT basis vectors. Thus, among the O_3 bases, one orthogonal basis is selected and then M_ν out of the K orthogonal vectors are selected for layer ν, which is one distinct feature from the SD basis vectors that the FD basis vectors can be independently selected for different layers. For simplicity, we assume $M_\nu = M$ for all layers.

For the coefficient matrix $\mathbf{W}_2$ corresponding to the selected SD/FD basis vector pairs, a subset of the $2LM$ coefficients comprising $\mathbf{W}_2$ is firstly selected for reporting, and the remaining 'weak' coefficients having close to zero amplitude values are set to zero. This is because a 'weak' coefficient does not contribute much to linear combination but incurs the same overhead as that of a 'strong' element. Furthermore, due to the quantization error, the contribution of the weak coefficients can be even inferior than no reporting case. Hence, only K_0 strong coefficients are considered to be quantized and reported among the $2LM$ coefficients in $\mathbf{W}_2$, and the rest $2LM - K_0$ coefficients are not reported and regarded as all zeros. Then, each selected 'strong' coefficient is decomposed into phase and amplitude, and they are quantized using respective codebooks. The phase is reported using either a 3-bit or 4-bit phase-shift keying (PSK) phase codebook: $\phi(N_p) = \{e^{\frac{j2\pi n}{2^{N_p}}} : n = 0, 1, \cdots, 2^{N_p} - 1\}$, where $N_p = 3$ or 4 and one of them can be configurable via higher-layer signaling. For the amplitude quantization, amplitude values are first normalized by the strongest amplitude and then the normalized amplitude values are quantized in a differential manner as $a = a^{(r)}a^{(d)}$, where $a^{(r)}$ and $a^{(d)}$ are a reference value and a differential amplitude value, respectively. The reference value is defined per polarization and is common for all coefficients of the corresponding polarization. The

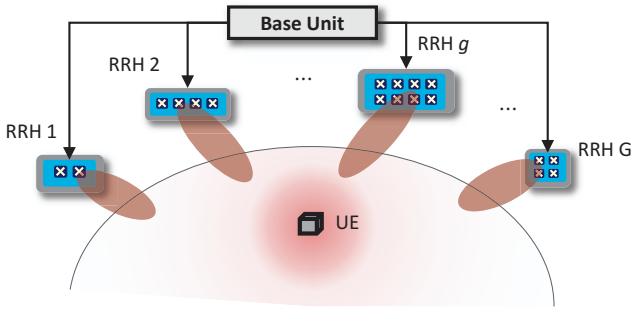

Figure 2. An example of distributed MIMO scenario.

reference value is set to 1 for the polarization associated with the strongest coefficient, and the other reference value for the other polarization is selected from a 4-bit amplitude codebook composed of equidistant points in [0,1] in 1.5 dB scale, i.e., $\{1, (\frac{1}{2})^{\frac{1}{4}}, (\frac{1}{4})^{\frac{1}{4}}, \cdots, (\frac{1}{2^{15}})^{\frac{1}{4}}\}$. The differential amplitude value for each coefficient is independently selected from a 3-bit amplitude codebook composed of equidistant points in [0,1] in 3 dB scale, i.e., $\{1, \frac{1}{\sqrt{2}}, \frac{1}{2}, \frac{1}{2\sqrt{2}}, \cdots, \frac{1}{8\sqrt{2}}\}$. Since the strongest coefficient is used to normalize other coefficients, its value is regarded as one and thus only the strongest coefficient index is reported using a strongest coefficient indicator (i.e., its amplitude/phase values do not have to be reported).

III. CSI Codebooks for Distributed MIMO

We consider a D-MIMO scenario where G RRHs are distributed over a cell and connected with a baseband unit capable of joint signal processing to perform coherent data transmission, as shown in Fig. 2. We assume that each RRH is equipped with a 2D active antenna array panel, and the equipped panels can be different across the RRHs. We also assume that $N_g = 2N_{1,g}N_{2,g}$ antenna ports at RRH $g = 1, ..., G$ are utilized where $N_{1,g}$ and $N_{2,g}$ are the numbers of antenna ports per polarization in the first and second dimensions, respectively, at RRH g. Following the same approach as that for centralized MIMO case, we can obtain the $N_g \times K$ dominant channel matrix $\mathbf{H}_g^{(\nu)}$ for each RRH g and stack the matrices for all RRHs to form the $N_{\text{all}} \times K$ whole channel matrix for the D-MIMO: $\mathbf{H}_{\text{DMIMO}}^{(\nu)} = [(\mathbf{H}_1^{(\nu)})^T (\mathbf{H}_2^{(\nu)})^T \cdots (\mathbf{H}_G^{(\nu)})^T]^T$, where $N_{\text{all}} = \sum_g N_g$.

In this section, we propose two CSI codebook design methods, namely 'decoupled' and 'joint' codebooks, tailored for the considered D-MIMO scenario to efficiently compress and represent $\mathbf{H}_{\text{DMIMO}}^{(\nu)}$. Both of the proposed codebooks are designed based on the Rel-16 Type-II CSI codebook. The 'decoupled' codebook is designed in a decoupled way that SD/FD beams are independently selected per RRH and inter-RRH components are newly added to perform coherent transmission from multiple RRHs. On the other hands, the 'joint' codebook is designed in a joint way that SD beams are independently selected per RRH but common FD beams are selected across RRHs. Note that the 'joint' codebook provides a more efficient CSI compression framework using the common FD beams whereas the 'decoupled' codebook offers a CSI feedback framework that can facilitate various/flexible features such as precoder/RRH cycling operations for diversity, or SB dynamic RRH subset selection (which will be described in Section IV-B). In the subsequent subsections, we provide the detailed descriptions of the two proposed CSI codebooks.

A. Decoupled codebook

The structure of the proposed decoupled codebook (called CB1 hereafter) can be expressed as:

$$\mathbf{H}_{\text{DMIMO}}^{(\nu)} \simeq \mathbf{W}_{\text{CB1}}^{(\nu)} = \begin{bmatrix} \mathbf{W}_{1,1}\mathbf{W}_{2,1}\mathbf{W}_{f,1}^H\mathbf{Q}_1 \\ \vdots \\ \mathbf{W}_{1,G}\mathbf{W}_{2,G}\mathbf{W}_{f,G}^H\mathbf{Q}_G \end{bmatrix}$$

where $\mathbf{W}_{1,g}$ and $\mathbf{W}_{f,g}$ are $N_g \times 2L$ and $K \times M$ basis matrices composed of SD and FD basis vectors, respectively, and $\mathbf{W}_{2,g}$ is an $2L \times M$ coefficient matrix corresponding to SD and FD basis vector pairs, for RRH $g = 1, \cdots, G$. Note that in CB1, $\mathbf{W}_{1,g}$, $\mathbf{W}_{2,g}$, and $\mathbf{W}_{f,g}$ follow the structures of $\mathbf{W}_1$, $\mathbf{W}_2$, and $\mathbf{W}_f$ in the Rel-16 Type-II codebook, respectively, and thus $\mathbf{W}_{1,g}$ $\mathbf{W}_{2,g}$, and $\mathbf{W}_{f,g}$ can be regarded as local CSI for the $N_g \times K$ channel at RRH g. Although the collection of the local CSI is sufficient to perform non-coherent joint transmission (JT) across RRHs, for coherent JT, additional component is needed to adjust phase mismatch and to compensate for power imbalance across RRHs. Thus, an inter-RRH component $\mathbf{Q}_g$ is added in CB1 to support D-MIMO to be capable of coherent JT from multiple RRHs, by resolving those phase mismatch and power imbalance issues. Here, $\mathbf{Q}_g$ is a $K \times K$ diagonal matrix with diagonal entries $q_{g,1}, \cdots, q_{g,K}$, each comprising a phase and an amplitude values for RRH $g = 1, \cdots, G$. That is, each $q_{g,k}$ can be further decomposed into $p_{g,k}$ and $a_{g,k}$ that are selected from the phase and amplitude codebooks.

B. Joint codebook

The proposed joint codebook is to support a framework that separately selects a SD basis per RRH and regards a whole SD basis matrix obtained by diagonally stacking SD bases for all RRHs as $\widetilde{\mathbf{W}}_1$ to be applied into the Rel-16 Type-II CSI framework. The structure of the codebook (called CB2 hereafter) can be represented as

$$\mathbf{H}_{\text{DMIMO}}^{(\nu)} \simeq \mathbf{W}_{\text{CB2}}^{(\nu)} = \widetilde{\mathbf{W}}_1 \widetilde{\mathbf{W}}_2 \widetilde{\mathbf{W}}_f^H$$

where $\widetilde{\mathbf{W}}_1 = \text{diag}[\mathbf{W}_{1,1}, \cdots, \mathbf{W}_{1,G}]$ is an $N_{\text{all}} \times 2GL$ SD basis matrix that diagonally stacks SD bases for all RRHs, $\widetilde{\mathbf{W}}_f$ is a $K \times M$ common FD basis matrix, and $\widetilde{\mathbf{W}}_2$ is a $2GL \times M$ matrix composed of the coefficients for the SD/FD basis vector pairs.

In CB2, a SD basis is independently selected per RRH, but compressed coefficients of $\widetilde{\mathbf{W}}_2$ are selected jointly across RRHs using a common FD basis $\widetilde{\mathbf{W}}_f$. The underlying principle of CB2 is to exploit the fact that channels across RRHs can be less spatially correlated than channels within each RRH whereas channels for all RRHs can be correlated across SBs since the same bandwidth associated with the configured SBs are used for all the modules with a given subcarrier spacing.

IV. Dynamic RRH Selection

The overhead of CSI feedback based on the two proposed codebooks can be large. For example, CB1 and CB2 require $2LMG + KG$ and $2LMG$ coefficients to be quantized and reported, respectively, which are the main portion of feedback overhead for CB1 and CB2. One practical approach to reduce the amount of feedback is to send CSI only for a subset of RRHs with dominant channel conditions, which we call dynamic RRH selection (DRS). Through DRS, the spatial diversity from different RRHs can be exploited and, at the same time, the overhead of CSI feedback can be opportunistically reduced by sending feedback for a subset of RRHs. DRS can be performed either at the BS or by the UE. When DRS is performed at the BS, the channel reciprocity is utilized by the BS to choose an optimal RRH subset based on measuring the UL channel at different RRHs. When DRS is performed by the UE, the selected RRHs are reported by the UE, e.g., as part of the CSI feedback.

In this section, we focus on DRS methods performed by the UE. Depending on granularity on frequency resources, we propose WB (frequency non-selective) and SB (frequency-selective) DRS methods. Since the UE selects a subset of RRHs and reports the CSI corresponding to the selected RRHs using a CSI codebook, a different level of constraints on designing the CSI codebook is needed. In the subsequent subsections, we provide WB and SB DRS methods with the usage of our proposed CSI codebooks followed by measurement and reporting to support DRS.

A. WB dynamic RRH selection

Once a UE receives DL reference signals such as CSI-RS transmitted from multiple RRHs in the D-MIMO network, the UE can determine which RRHs are chosen based on a certain criterion. For standard specification potentially including signaling between the BS and UE, the criterion is preferred to be simple yet effective. We propose the following criterion for the UE to perform WB DRS: select the R best RRHs in the decreasing order of their reference signal received power (RSRP) values, where $R \geq 1$ is determined as the lowest positive integer such that the sum of the ordered RSRPs for the R best RRHs is greater than or equal to ρP_{sum}, where $\rho \leq 1$ and P_{sum} is the total sum of RSRPs for all RRHs in the D-MIMO network. In other words, the criterion allows the selected set S of RRHs to contain the best RRHs so that their total sum RSRP becomes greater than or equal to the ρ portion of the total sum of RSRPs for all RRHs. Note that since ρ indicates a fraction, it can be defined in $[0, 1]$, and thus it is easy to define signalling to support the WB DRS in the standards. Note also that setting $\rho = 0$ and 1 reduce to the best RRH selection case and all RRH selection case, respectively, whereas setting $\rho \in (0, 1)$ implies in-between the best and all RRH selection cases. Depending on the value of the parameter ρ, the UE can dynamically/opportunistically collect a large fraction of the total RSRP by selecting the dominant RRHs, and at the same time, minimize potential interference from non-dominant or 'weak' RRH(s) to other UEs in the network.

After WB DRS, the UE generates the CSI using CB1 or CB2 and reports the CSI to the network. Both CB1 and CB2 can be directly applied to the selected set S of RRHs.

B. Frequency-selective dynamic RRH selection

To improve DRS performance, we may consider frequency-selective (or SB) DRS wherein the UE selects a subset of RRHs per SB or a finer granularity than WB. Since the channel qualities can vary across frequency resources within the carrier bandwidth, an optimal subset of RRHs for the UE can be different across SBs. Similar to the WB DRS method, we can adopt the same criterion with parameter ρ for the UE to select RRHs per SB, achieving frequency-selective DRS. Compared to the WB DRS method wherein both of CB1 and CB2 can be applicable, however, the SB DRS cannot be applied directly to CB2 due to the fact that a different set of SBs can be chosen for different RRH. The different sets of SBs chosen for different RRHs can result in dimension mismatch in FD basis vectors (parameter K) across RRHs, which is inconsistent with the common FD beam vectors $\mathbf{W}_f$ selection across RRHs, as required in CB2. Thus, a CB1-based approach would be more appropriate to support the SB DRS method.

Let $S_{\text{SB}}(g)$ and $S_{\text{RRH}}(k)$ be a set of selected SBs for RRH g and a set of selected RRHs for SB k, respectively. Then, the CB1-based approach to support the SB DRS can be decomposed into two components.

Component 1: For each RRH g, we can have $\mathbf{H}^{(\nu)}_{\text{DMIMO}}(S_{\text{SB}}(g))$ which is the $N_g \times |S_{\text{SB}}(g)|$ submatrix of $\mathbf{H}^{(\nu)}_{\text{DMIMO}}$ composed of the rows corresponding to RRH g and the columns corresponding to the elements in $S_{\text{SB}}(g)$. For matrix $\mathbf{H}^{(\nu)}_{\text{DMIMO}}(S_{\text{SB}}(g))$ of each RRH g, we use the same CSI structure of Rel-16 Type-II CSI with replacing K by $|S_{\text{SB}}(g)|$, that is, $\mathbf{H}^{(\nu)}_{\text{DMIMO}}(S_{\text{SB}}(g)) \simeq \mathbf{W}_{1,g}\mathbf{W}_{2,g}\mathbf{W}^H_{f,g}(S_{\text{SB}}(g))$, where $\mathbf{W}_{f,g}(S_S B(g))$ is a $|S_{\text{SB}}(g)| \times M$ FD basis matrix.

Component 2: Inter-RRH phase/amplitude values are needed for each SB where multiple RRHs are selected, and are hence reported. For the remaining SBs where only on RRH selected, there is no need for inter-RRH phase/amplitude reporting.

Using the two components, the UE can generate the CSI for the SB DRS method and report it along with the information on the sets of selected SBs for RRHs.

C. Measurement and reporting for dynamic RRH selection

For dynamic RRH selection, a UE receives CSI-RS sent from each RRH, and measures channel qualities between the UE and each RRH. Note that a CSI-RS resource can act as a channel measurement resource (CMR) or an interference measurement resource (IMR) depending on the RRH selection hypothesis. For example, a CSI-RS resource transmitted from an RRH acts as a CMR if the corresponding RRH is selected for CSI reporting, and acts as an IMR, otherwise. Once the UE performs DRS and determines the selected and unselected sets S and S^c, the UE can compute the SINR based on the selected and unselected sets, i.e., $\frac{\sum_{i \in S} P_i}{\sum_{j \in S^c} P_j + I + N}$ where P_i is the RSRP

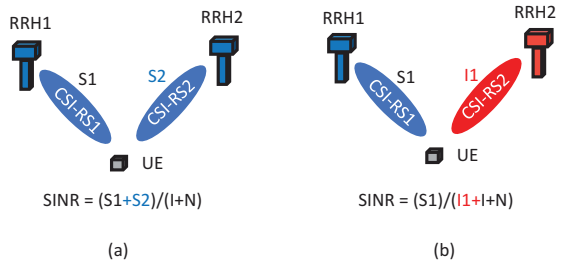

Figure 3. Measurement and reporting depending on dynamic RRH selection.

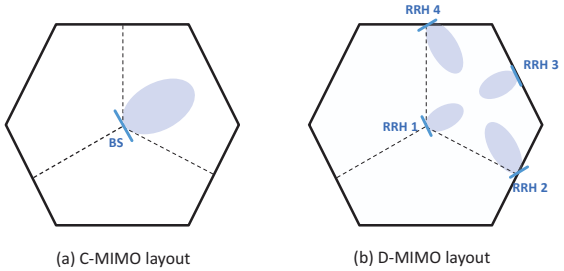

Figure 4. Layouts of (a) C-MIMO and (b) D-MIMO for SLS evaluations.

for RRH i. The SINR computed by UE after performing DRS can be reported along with the CSI corresponding to the selected RRHs.

An example is illustrated in Fig. 3, wherein there are two RRHs (RRH1 and RRH2) transmitting CSI-RSs (CSI-RS1 and CSI-RS2 respectively). Two cases of the RRH selection are shown. In Fig 3 (a), both RRHs are selected, and thus both CSI-RSs act as CMRs, and the SINR value can be expressed as $\text{SINR} = (S1 + S2)/(I + N)$ where $S1$ and $S2$ are desired signal power from RRH1 and RRH2, respectively, and I and N are interference power and noise power, respectively. In Fig. 3 (b), RRH1 is selected, and thus CSI-RS1 acts as a CMR and CSI-RS2 acts as an IMR, and the SINR value can be expressed as $\text{SINR} = (S1)/(I2 + I + N)$ where $I2$ is the interference power from RRH2. As illustrated, CSI-RS from RRH2 acts as a CMR in Fig. 3 (a) and as an IMR in Fig. 3 (b). We can regard $I2$ as an "inter-RRH interference" in Fig. 3 (b).

V. System-Level Simulation Results

To perform SLS for D-MIMO scenarios, we consider a hexagonal layout for D-MIMO deployment, as shown in Fig. 4, where each hexagonal comprises three sectors. Compared to the conventional layout for centralized MIMO (C-MIMO) as shown in Fig. 4(a), three additional RRHs are deployed in each sector to form an D-MIMO network, as shown in Fig. 4(b). The three additional RRHs in each sector are located at the midpoints between the centers of its associated site and neighboring sites, respectively. Each RRH's tilting angle is facing towards the center region of the associated sector. For simplicity, it is assumed that the antenna structure is the same for each RRH. To simulate low frequency band scenarios, the 3GPP rural macro (RMa) channel model with the center frequency of 700 MHz is adopted, where the inter-site distance is assumed to be 1.7 km. A total of 57 sectors (19 hexagonal sites) in a two-tier deployment is considered and up to 30 UEs are randomly dropped in each sector. A non-full-buffer traffic model is assumed. Due to low frequency band and small UE form factor relative to the wavelength of carrier frequency, only two antenna elements is assumed at each UE. Up to four layers of MU-MIMO is considered for MU scheduling at the BS in each sector.

To illustrate the benefit of D-MIMO, the average user perceived throughput (UPT) gains of D-MIMO with the proposed CB1, CB2, and ideal CSI are compared with those of C-MIMO with Rel-16 Type-II CSI and ideal CSI, where the ideal CSI is based on the perfect knowledge of dominant eigenvectors at the BS. Fig. 5 shows the corresponding performance result for the case when the same total number of antenna elements is utilized for both C-MIMO and D-MIMO. In this case, we considered the three antenna structures comprising 64, 16, and 8 antenna elements, respectively, in total for both C-MIMO and D-MIMO. The antenna elements are virtualized to form CSI-RS ports so that $N = 32, 8$, and 8 CSI-RS ports are utilized for C-MIMO whereas $N = 16, 8$, and 8 CSI-RS ports are utilized for D-MIMO (i.e., $\bar{N} = N_g = 4, 2$, and 2 ports per RRH in D-MIMO). As shown in Fig. 5, it is validated that D-MIMO with the proposed codebooks yields significant average UPT gains over the C-MIMO – up to 13%, 23%, and 44% for low resource utilization (RU), medium RU, and high RU, respectively, even when the same total number of antenna elements is utilized for both C-MIMO and D-MIMO. It is shown that the proposed CB1 for D-MIMO yields worse performance than the proposed CB2 for D-MIMO. This is because the disjoint codebook structure of CB1 limits the quality of the CSI. Also, it can be observed that the average UPT gain of D-MIMO over C-MIMO starts decreasing as the total number of antenna elements increases. The reason is that for each antenna case, the relative average UPT gains are normalized by the performance of C-MIMO Rel-16 CB corresponding to the antenna case, and the performance of C-MIMO and D-MIMO with a larger number of antenna elements achieves better throughputs that are closer to the performance limit determined by the modulation and coding scheme, which turns out the relative average UPT gain becomes reduced.

Fig. 6 shows the performance results for the case when the same number of antenna elements is utilized per RRH for both C-MIMO and D-MIMO, i.e., D-MIMO has 4 times more antenna elements than C-MIMO. In this case, we considered the two antenna structures comprising 16 and 8 antenna elements, respectively, per RRH for both C-MIMO and D-MIMO. In other words, 64 and 32 antenna elements in total are considered for the D-MIMO. The antenna elements are virtualized to form CSI-RS ports, $N = 16$ and 8 CSI-RS ports are utilized for C-MIMO whereas N=16 and 16 CSI-RS ports are utilized for D-MIMO (i.e., $\bar{N} = N_g = 4$ and 4 ports per RRH in D-MIMO).

As shown in Fig. 6, similar trends are observed, i.e., the average UPT gain of D-MIMO over C-MIMO starts increasing

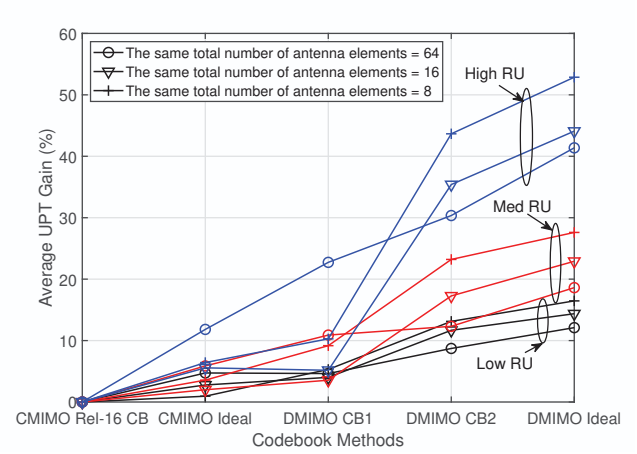

Figure 5. Average UPT gain of D-MIMO over C-MIMO in the case of the same total number of antenna elements for C-MIMO and D-MIMO.

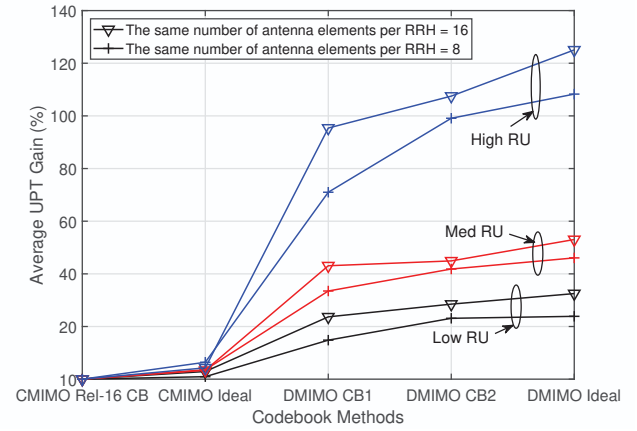

Figure 6. Average UPT gain of D-MIMO over C-MIMO in the case of the same number of antenna elements per RRH, i.e., 4x more than C-MIMO.

as RU increases. Also, it is shown that the D-MIMO with the proposed codebooks yields huge average UPT gains over the C-MIMO – up to 32%, 47%, 118%, for low-, med-, and high-RU, respectively. This result shows that the D-MIMO with the proposed CSI codebooks has a great potential to considerably improve the system performance in low band scenarios by overcoming the practical constraints such as the infeasibility of co-locating a large number of antenna elements at one site.

Finally, we evaluate the performance of the proposed D-MIMO codebooks with and without the feature of DRS. Fig. 7 considers the same scenario as the one considered in Fig. 5 with the high RU for the D-MIMO. For the DRS, the UE chooses the best RRHs whose sum signal power occupy more than the ratio ρ of the total sum signal power of all RRHs, and reports the CSI corresponding to the selected RRHs only based on the proposed codebooks. As shown in Fig. 7, adopting the feature of DRS yields significant performance gain (up to 23%) over the no RRH selection case, and additionally, reduces the feedback overhead significantly as depicted via yellow lines. This is because the DRS allows the UE to report the CSI corresponding to the best RRHs in an opportunistic manner so as to extract the most of the desired signal power

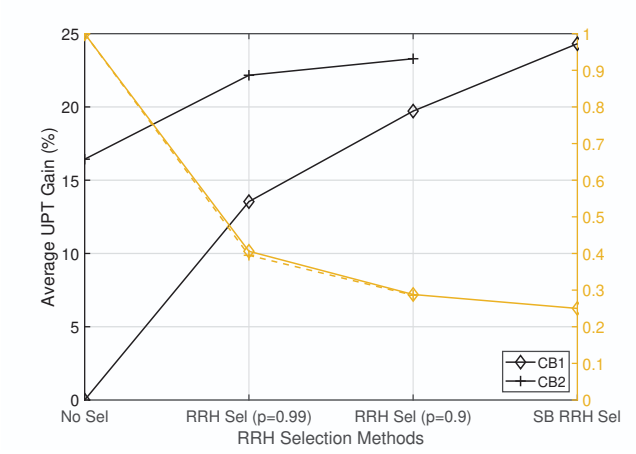

Figure 7. Performance of the proposed codebooks w.r.t. DRS methods.

(up to the ratio ρ) and to exclude the RRHs having 'weak' channel qualities, which in turn could reduce undesirable interference to other cells. Furthermore, the SB DRS with CB1 yields further performance gain (approx. 5% additional gain) by exploiting the frequency-selective of RRH selection.

VI. Conclusion

In this paper, CSI codebooks are proposed to facilitate the CSI feedback tailored for the D-MIMO system. In addition, WB and SB DRS methods are proposed to reduce the amount of feedback overhead and to obtain performance gain by allowing the UE to report the CSI corresponding to the best RRHs in an opportunistic manner. The performance gains of the D-MIMO with the proposed CSI codebooks and DRS methods are demonstrated through SLS evaluations under realistic scenarios by comparing with the centralized MIMO based on the latest (Rel. 16) 5G NR CSI feedback paradigm. It has been shown that the proposed codebooks and DRS methods have a great potential to considerably enhance the D-MIMO system performance in low band scenarios.

References

[1] 3GPP Technical Report, TR 38.913, "Study on scenarios and requirements for next generation access technologies."
[2] 3GPP Technical Specification, TS 38.214 v16.5.0, "NR Physical Layer Procedure for Data."
[3] 3GPP RAN, RP-202024, "Further enhancements on MIMO for NR." Samsung, 2020.
[4] M. S. Rahman et al., "MIMO in low frequency bands," *submitted to IEEE Communications Standards Magazine*, Jun. 2021.
[5] W. Choi et al., "Downlink performance and capacity of distributed antenna systems in a multi-cell environment," *IEEE Transactions on Wireless Communications*, vol. 6, no. 1, Jan. 2007.
[6] H. Q. Ngo et al, "Cell-free massive MIMO versus small cells," *IEEE Transactions on Wireless Communications*, vol. 16, no. 3, Mar. 2017.
[7] E. Bjornson et al, "Massive MIMO: ten myths and one critical question," *IEEE Transactions on Wireless Communications*, vol. 54, no. 2, Feb. 2016.
[8] ——, "Massive MIMO is a reality – what is next? five promising research directions for antenna arrays," *Digital Signal Processing*, vol. 94, Nov. 2019.
[9] Y. Huang et al, "Multi-panel MIMO in 5G," *IEEE Communications Magazine*, vol. 56, no. 3, Mar. 2018.
[10] M. S. Rahman et al., "CSI feedback based on space-frequency compression," in *IEEE 17th Annual Consumer Communications & Networking Conference (CCNC)*, Jan. 2020.